Taylor & Francis Word Template for journal articles

C. L. Lorenz[a], A. B. Spaeth[a], C. Bleil de Souza[a] and M. S. Packianather[b]

[a]Welsh School of Architecture, Cardiff University, Cardiff, U.K.; [b]School of Engineering, Cardiff University, Cardiff, U.K.

Lorenzc4@cardiff.ac.uk

Artificial Neural Networks for Parametric Daylight Design

In parametric design environments, the use of Artificial Neural Networks (ANNs) promises greater feasibility than simulations in exploring the performance of solution spaces due to a reduction in overall computation time. This is because ANNs, once trained on selected input and output patterns, enable instantaneous predictions of expected outputs for new unseen input in the recall mode. In this study, ANNs were trained on simulation data to learn the relationship between design parameter and the resulting daylight performance. The ANNs were trained with selected input-output patterns generated from a reduced set of simulations in order to predict daylight performance for a hypercube of design solutions. This work demonstrates the integration of ANNs in a case study exploring designs for the central atrium of a school building. The study discusses the obtained design results and highlights the efficacy of the proposed method. Conclusions are drawn on the advantages of brute-force based daylight design explorations and the potential of an ANN-integrated design approach.

Keywords word: Daylight analysis in parametric design, Neural Networks in parametric design, Daylight in atriums, Neural Networks in early design stages

1. Introduction

This study aims to improve the feasibility of daylight assessments in parametric design environments. It specifically focuses on proposing the use of Artificial Neural Networks (ANNs) to streamline daylight results to better explore design solutions by giving faster performance feedback to designers.

1.1 Climate-based daylight modelling

As part of the wider discussion on sustainable building design, daylighting has been found imperative for occupant well-being and energy savings (Bodart and De Herde 2002; Figueiro et al. 2017; Veitch, Christoffersen, and Galasiu 2013). Daylight is an interesting design factor, given its significant impact on retail sales performance (Heschong, Wright, and Okura 2002), as well as school and work achievement (Heschong et al. 2012; Maesano and Annesi-Maesano 2012). Backed by research determining a daylight threshold to ensure

occupant comfort and satisfaction, specifically in school-buildings (Heschong et al. 2012), dynamic climate-based daylight modelling (CBDM) found its adaptation as a requirement for applications to the PSBP (Priority Schools Building Program) in the UK in 2012 (EFA 2014) as well as in European and British building standards (BS EN 17037:2018). Thus, the focus in both research and practice has turned away from the standard Daylight Factor (DF) metric towards climate-based daylight metrics.

Climate-based daylight metrics are calculated over the course of a whole year, typically in hourly or minutely intervals for times the building is occupied. In comparison to the point-in-time DF metric, which is usually calculated under overcast sky conditions and without considering orientation, solar altitude or effects of shading (Reinhart, Mardaljevic, and Rogers 2013), CBDM gives an aggregated measure of daylight for the prevailing conditions at the site and is intended to evaluate the overall daylighting potential of a building (Mardaljevic 2008). However, the calculation of climate-based daylight metrics is computationally intensive and can take up several hours.

1.2 Brute-force approach in parametric environments

Time-intensive CBDM can prove to be a challenge when assessing the daylight performance for numerous scenarios, especially in parametric design environments when designers aim to push for daylight optimisation. Parametric design is an environment which enables designers to go from solution to design. If, on the one hand, a parametric design environment offers the opportunity to improve building performance via automated and systematic searches and/or the use of optimisation algorithms, the climate-based simulations on these models, on the other hand, becomes increasingly time-consuming with every design solution that is being simulated (Eltaweel and Su 2017). Therefore, the number of possible solutions, i.e. the size of the design space, constitutes a limitation to such processes. In effect, this limits the number of design variables, which are the number

of choices a designer can make with the objective of improving performance (Tresidder 2014).

A full parametric analysis of all combinations of design variables, also known as the brute-force search method, allows the user to engage with results of the entire design solution space. Such method is therefore suitable for developing design guidelines, and further enables designers to combine optimisation results according to their own judgement (Samuelson et al. 2016). This study relies on the brute-force approach to provide performance feedback on all possible solutions of the design space. Brute-force was deemed essential, firstly because causal relationships can be learned from the trends, and secondly because this provides designers with the freedom of choice to make informed decisions. Thus, even if an optimal solution is rejected, the decision is informed, i.e. the consequences are known.

The brute-force approach however, as an exhaustive search method, is especially computationally intensive. At this point, the introduction of ANNs offers promising possibilities to facilitate design exploration as they significantly shortcut the large number of simulations necessary, yet still deliver performance feedback on all design solutions. This paper proposes an ANN-integrated design approach to produce quasi real-time daylight assessment of climate-based metrics. It illustrates this approach through testing it in a case study school building for different types of atrium designs.

1.3 Application of ANNs in daylighting

The concept of ANN-based predictive modelling as replacement for cycle-by-cycle simulations has been implemented in various fields of performance analysis, either in optimisation or to efficiently explore design solution spaces (Ipek *et* al. 2006; Forrester and Keane 2009; Magnier and Haghighat 2010; Zhao and Magoulès 2012). In the field of

daylight design, previous work can be found for daylight and energy consumption, optimisation of thermal and visual comfort, blind position and control as well as predictions of daylight factors and daylight illuminance.

ANNs were used to predict the energy consumption for lighting (Wong, Wan, and Lam 2010). The models had a high predictive power and the errors ranged from -0.2% to +3.6% for predictions on electricity use. Fonseca, Didoné and Pereira (2013) also proposed ANNs as prediction models to assess the impact of daylighting on electric energy consumption. The models delivered high accuracies during cross-validation, but their validity had yet to be determined for predictions on unseen cases. On the optimization of an integrated daylighting and HVAC system, ANN predictions were integrated into a genetic algorithm to minimise energy consumptions while satisfying thermal and visual comfort (Kim, Jeon, and Kim 2016). ANN-based methods have also been tested for real-time feedback, specifically for automated blind and lighting control. Coley and Crabb (1997) proposed the application of ANNs to remotely control electric lighting by predicting indoor illuminances at chosen points based on external measurements of vertical illuminance. Similarly, Hu and Olbina (2011) used ANNs to predict optimal slat angles for split blinds to achieve designed indoor illuminances. Neuro-fuzzy systems have also been suggested for blind position control (Bhavani and Khan 2009).

Conraud-Bianchi (2008) trained an ANN model on 200 simulation cases in order to predict the average daylight factor across a series of points for 50 new cases. The achieved relative errors were lower than 2.5%. In another optimisation study, Zhou and Liu (2015) trained ANN models and support vector machines on simulation data in order to predict hourly results for the climate-based UDI (Useful Daylight Illuminance) metric. The model was limited to binary output that determined whether daylight levels fell within a specific illuminance range.

To the best of the authors' knowledge, there are no studies that use ANNs to predict annual aggregated climate-based metrics (neither DA nor sDA) in parametric design environments. The referenced works predict daylight for different climate conditions and sun positions, i.e. ANNs were trained with climate data as part of the training data. In comparison, this work collapses the time-series entirely, i.e. it is assumed that ANNs can emulate daylight contributions of an entire year. The ability of ANNs to predict climate-based metrics for design alterations and varying design scenarios, in the context of the specific case study explored in this paper, has been tested successfully (Lorenz and Jabi 2017; Lorenz *et* al. 2018).

2. Methodology

In order to test the use of an ANN-integrated design approach to produce quasi real-time daylight assessment using CBDM, this paper explores different atrium design alternatives for the Katharinen School in Hamburg (Germany). The building is located in a dense urban area with surrounding buildings obstructing the natural access to daylight (Figure 1). Therefore, the atrium provides a means of bringing additional daylight into the building, making it a viable design feature for optimisation.
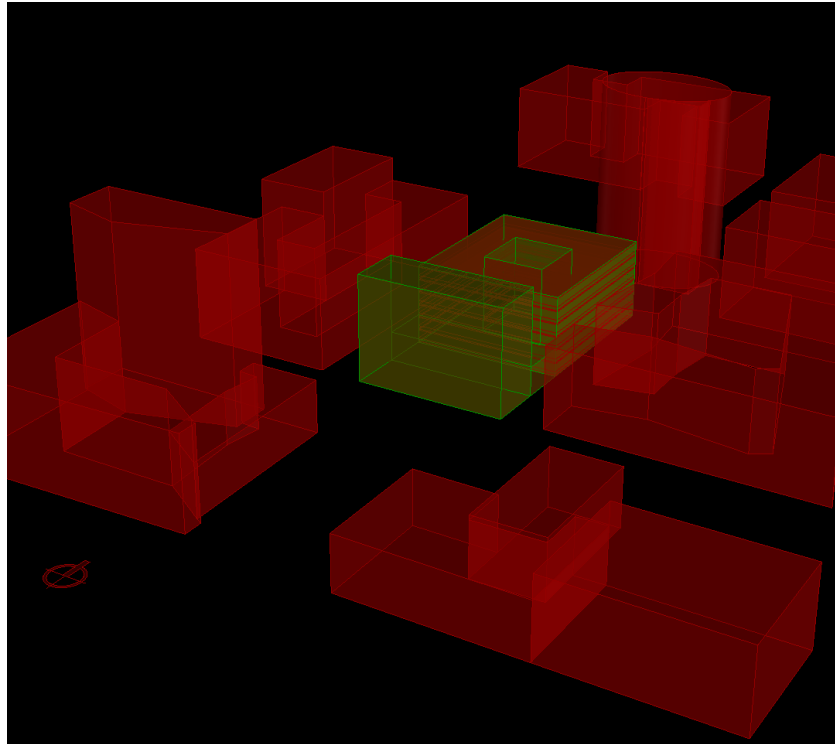
Figure 1. Grasshopper model of the Katharinen School (highlighted in green) with its central atrium and surrounding buildings

Figure 2 illustrates the process used in the exploration of the solution space. A set of design alternatives were generated, and a small number was selected and passed to a daylight simulation engine. Daylight simulations were conducted from which data describing the design changes as well as the corresponding daylight results were extracted. Subsequently, ANN models were developed by providing the extracted data to a particular network topology to undergo supervised training. Once trained, these ANN models were validated and integrated into the parametric model to assess the daylight performance of all design solutions in the design space. The following sections detail the processes described in Figure 2, from the modelling of the solution space to the training and validation of ANN models.
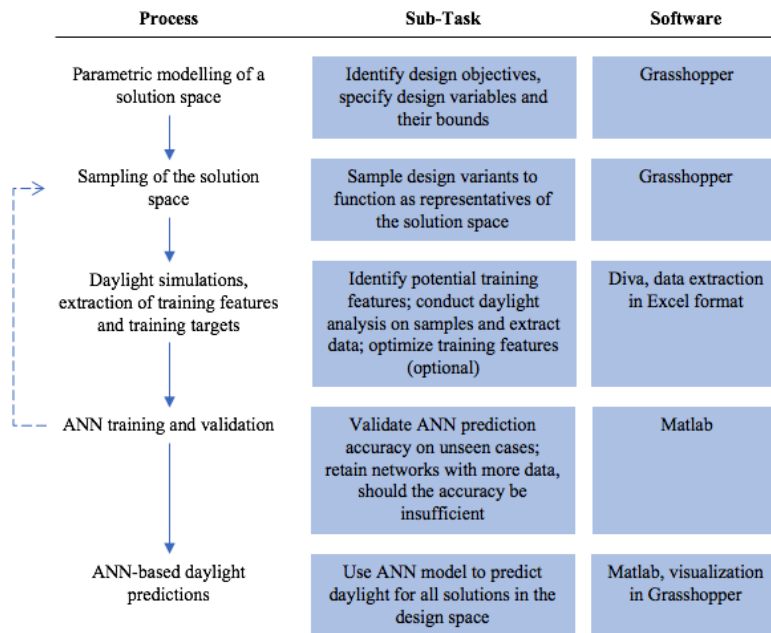
Process	Sub-Task	Software
Parametric modelling of a solution space	Identify design objectives, specify design variables and their bounds	Grasshopper
Sampling of the solution space	Sample design variants to function as representatives of the solution space	Grasshopper
Daylight simulations, extraction of training features and training targets	Identify potential training features; conduct daylight analysis on samples and extract data; optimize training features (optional)	Diva, data extraction in Excel format
ANN training and validation	Validate ANN prediction accuracy on unseen cases; retain networks with more data, should the accuracy be insufficient	Matlab
ANN-based daylight predictions	Use ANN model to predict daylight for all solutions in the design space	Matlab, visualization in Grasshopper

Figure 2. ANN-integrated approach for daylight assessment of design exploration

2.1 Design solution space

Design solutions were explored for the central atrium with the aim of bringing more daylight into its adjacent spaces on the lower floors. Design alterations were proposed for the atrium geometry, orientation and Window-to-wall ratios (WWR) of the atrium walls (Table 1).

Table 1. Design variables used in the proposed design alterations to improve daylight conditions

Variable Category	Design Variable	Number of Choices	Maximum and Minimum Bounds
Atrium geometry	Atrium base dimension	6	56.25 to 225 m^2
Atrium orientation	Atrium top and atrium base location	9	Units along x-axis: - 4 to 4 4 to - 4
Atrium well facade	WWR distribution	3	WWR ratios top to bottom floors:

	50, 60, 70, 80, 90, 100% WWR
	20, 35, 50, 65, 80, 100% WWR
	20, 30, 40, 50, 60, 100% WWR

Since splaying the atrium well walls increases the visible sky component and the usable floor area and the resulting 'V' shaped atrium geometry has the potential to allow for deeper daylight penetration into atrium adjacent spaces (Erlendsson 2014), the architectural model was parametrised by scaling the atrium base dimension with a factor between 0.5 and 1, in increments of 0.1. This produced 6 possible solutions with atrium base dimensions of 56.25, 81, 110.25, 144, 182.25 and 225 m^2, respectively.

On top of these previous first set of variations, the orientation and exposure of the facades of the atrium well to sunlight were varied by moving the atrium base and atrium top in opposite directions along the x-axis positioned at the centre of the atrium. The atrium base was moved between -4 to 4 m and the atrium top between 4 to -4 m, in increments of 1 m, producing 9 solutions. Taken together, this resulted in a 9 by 6 matrix with 54 possible combinations (Figure 3).
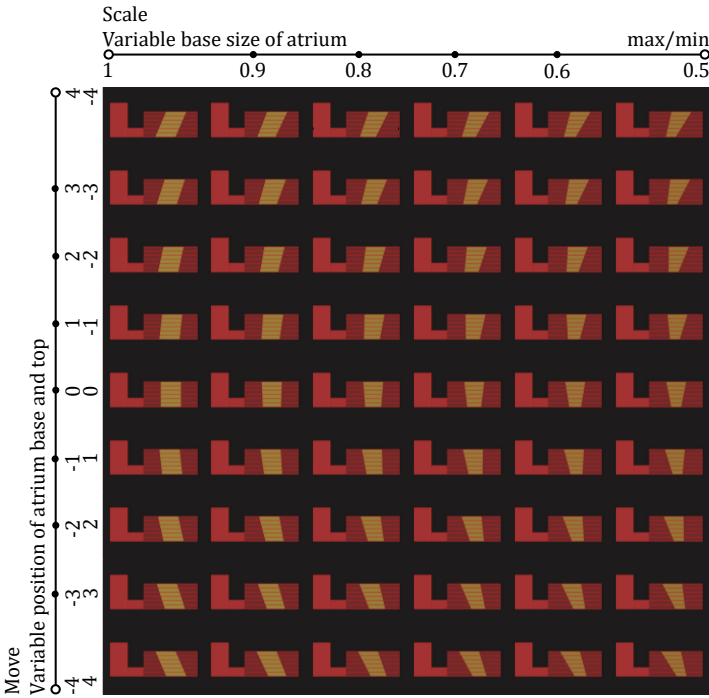

Figure 3. Design space of 54 possible combinations after adding two different types of parametric variations (splaying and sunlight orientation). The images show the east section of the grasshopper model.

The solution space of 54 variants was extended by altering the glazing distribution across different floor levels. Aschehoug (1992) suggested that a WWR distribution of 50, 60, 70, 100% from top to bottom floors works best for a 4-storey building as this increases the daylight reflected component. For a 5-storey building with a square atrium, Cole (1990) found the distribution of 20, 40, 60, 80 and 100% (from top to bottom) to be most effective in increasing daylight levels on the lower floors. In contrast, Samant (2017) who also investigated WWR distribution for a 5-storey building with square atrium, showed that a WWR distribution starting from 50-60% WWR on the top floors performed better than WWR ratios of 20-40%. This is because the drop in daylight levels on upper floors as a result of reducing the glazing area to 20% WWR was higher than the achieved increase of daylight levels on lower floors, making the change less worthwhile.

Based on these findings, three WWR distribution options were selected for the central atrium, as indicated in the last column of Table 1, with each of them applied to the 54 solutions increasing the size of the solution space to be investigated to 162 variants. The reflectivity of atrium well wall was set to a diffuse reflectance of 80%.

2.2 Sampling of the design space

ANNs require training data to learn relationships between design parameters and corresponding daylight performance so they can 'mimic' daylight simulations. The authors randomly extracted 45 design solutions out of the total 162. Although intelligent sampling methods exist, random sampling of simulation data has been found to yield good results (Ipek *et* al., 2006) and was therefore used in this study for simplification purposes.

2.3 Daylight simulation

The two climate-based metrics Daylight Autonomy (DA) and spatial Daylight Autonomy (sDA) were used to assess the daylighting potential of the design variants. DA denotes the

number of occupied hours in a year in which an illuminance threshold, typically set to 300 lux for office work, can be maintained by daylight alone (Reinhart and Walkenhorst 2001). sDA is derived from the DA metric and describes the percentage of work plane area that can meet the $DA_{300\ lux}$ threshold for 50% of occupied hours. Specifications for the sDA metric have been set to 50% (IES LM-83-12; EFA 2014).

Daylight simulations were run in Diva[1] for Grasshopper, a Radiance-based and validated simulation tool (McNeil and Lee 2012). The work plane was set to a height of 0.8m and sensor points were distributed with 0.6m spacing from each other. The radiance simulation parameters are listed in **Error! Reference source not found.**2.

Table 2. Radiance simulation parameters

Ambient bounces (ab)	6
Ambient divisions (ad)	2046
Ambient resolution (ar)	500
Ambient super-samples (as)	500
Ambient accuracy (aa)	0.1

2.4 Feature extraction

The training data set used as input for the network consisted of 45 randomly sampled simulated design variants. Training samples comprise the input features of each design variable and its corresponding DA output values. Input features were extracted for all sensor points for which DA levels were simulated. These extracted features describe changes occurring in the architectural model. A list of extracted input features is given in **Error! Reference source not found.**3. They were further optimised using sequential

---

[1] *Di*va. *Solemma LLC*. Available at: http://solemma.net/Diva.html (accessed Oktober 21, 2019).

feature selection in order to improve prediction accuracies and reduce overall training time.

Table 3. Data extracted to train the ANN models

Sensor Point Specific Training Features	Value Range	Design Variable Specific Training Features	Value Range
x, y coordinates of sensor point (2 features)	0.12 to 35.5 24.9 to 64.7	Splay angles of atrium well (4 features)	58.4 to121.9° 52.2 to113.2° 58.4 to 121.9° 52.2 to 113.2°
Distance to north, south, east, west façade (4 features)	0.1 to 39.9 m 0.1 to 35.5 m 0.1 to 39.9 m 0.1 to35.5 m	Glazing area at simulated floor level (4 features, one for each atrium well wall)	8.2 to 42.3 m^2 8.2 to 46.1 m^2 8.2 to 42.3 m^2 8.2 to 46.1 m^2
Distance to closest atrium point (1 feature)	0 to 24.4 m	Glazing area across all floors (1 feature)	350.2 to 1091.1 m^2
Direction of closest atrium point (1 feature)	0 to 360°	Dimension of the daylight calculation grid (1 feature)	1199 to 1364.1 m^2
Distance to atrium centre (1 feature)	2 to 29.8 m	Atrium dimension at the height of calculation grid (1 feature)	60 to 225 m^2
Direction of atrium centre (1 feature)	350.2 to 1091.1 m^2	Dimension of the atrium base area (1 feature)	56.3 to 225 m^2
Location of sensor point inside or outside atrium well (1 feature)	0, 1	WWR at 2nd/ 3rd/ 4th/ 5th/ 6th floor (1 feature)	20, 20, 50% (6th) 30, 35, 60% (5th) 40, 50, 70% (4th) 50, 65, 80% (3rd) 60, 80, 90% (2nd)

2.5 ANN training

ANNs process and pass information over a system of neurons with varying connection strengths. *Feed-forward neural networks* are typically arranged in an input layer that receives the training data, one or more hidden layers that develop a pattern of connections to replicate functions and an output layer that delivers the predictions (Figure 4). Before training, the extracted input features are passed to the neurons of the input layer, and the corresponding DA results to the neuron in the output layer. Training takes place in epochs, during which the networks adjust the connection strengths between neurons in order to minimize the mean squared error (MSE) between the simulated and predicted result. The MSE was observed for the training data which was subdivided into a training, test and

validation subset at the ratio of 65:15:20. The training subset was used to measure training accuracy, the validation subset was used to introduce early-stopping and prevent overfitting, and the test subset was used to measure generalisation capability. Gradient descent-based backpropagation training was employed in conjunction with the Levenberg-Marquardt algorithm to adjust the connection strengths (Marquardt 1963). A custom script was used to optimize the number of neurons in the hidden layers of the network. Each ANN configuration was trained 10 times in parallel, with randomised initial weight settings and randomised data in each ratio. Finally, the output of the 10 ANN models with the lowest overall MSE was averaged to further improve the robustness of predictions. The specific ANN training settings are detailed in Table 4.
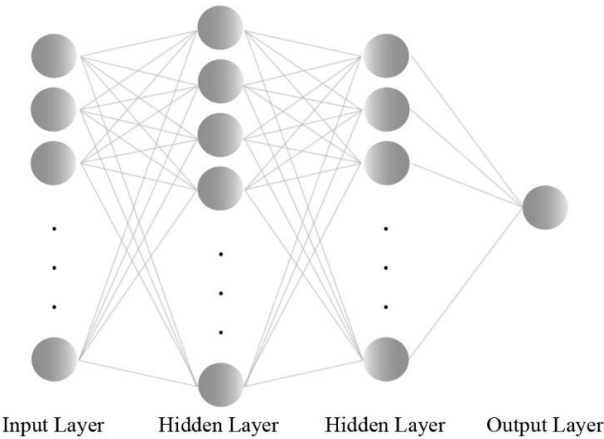

Figure 4. Simplified representation of an ANN architecture with one input layer, two hidden layers and one output layer. The features described in Table 3 were passed to the input layer, and the corresponding DA to the output layer.

Table 4. ANN training settings

Initial Mu	1
Mu decrease factor	0.8
Mu increase factor	1.5
Number of training epochs	200
Maximum number of validation failures	6

2.6 ANN validation

In order to determine that the ANN models could predict the daylight performance for the entire design landscape, their accuracy was validated against simulation results in a previous paper (Lorenz *et* al. 2019). The ANN models were able to predict the daylight performance after being trained with data from 36 out of 162 simulations. The trends in performance were also correctly identified, as the ANN models successfully predicting the ranking of options in accordance with the order of the simulated results. In this study, the number of simulations from which training data was extracted was increased to 45 out of 162 simulations. Additionally, a network architecture with two hidden layers was used. The resulting absolute difference between predicted and simulated daylight levels was 0.53 DA and 0.28 sDA on average on a validation data set constituent of 21 unseen simulations or 13% of the solution space. The root mean squared error was 0.86 DA and 0.33 sDA. Thus, it was concluded that the ANNs could deliver high prediction accuracies for this scenario.

3. Results and discussion

The validated ANN models were used to obtain the DA and sDA results for all atrium designs in the solution space. As Lorenz *et* al. (2019) focused on the validation of results, this paper focuses on the value of daylight results that can be obtained by such a facilitated sDA acquisition process. Results are presented in terms of spatial Daylight Autonomy (sDA) for the ground, third and top floors with a detailed analysis of how different WWR, orientations and geometries affect daylight performance. Figure 5a provides a graphic structure to read the results. Figure 5b illustrates all 9 orientations and Figure 5c shows where atrium splay angles are measured. Both aid understanding the influence of atrium well orientation discussed in the upcoming results sections. Patterns, trends and magnitude of results were assessed in terms of how each different design variable contributed to sDA

changes.

SDA results in atrium adjacent spaces ranged overall between 21 and 29 % on the
ground floor, 37 and 46 % and on the third floor and between 75 - 95% on the top floor
(Figure 6). When the atrium well area is included to the analysis of ground floor, sDA
range increases overall from 24 to 41%. Differences in daylight performance among these
three floors vary between 7% (for the ground floor) up to 20% (for the top floor) for all 162
atrium design solutions. Such a change justifies deeper investigation in cause and effect
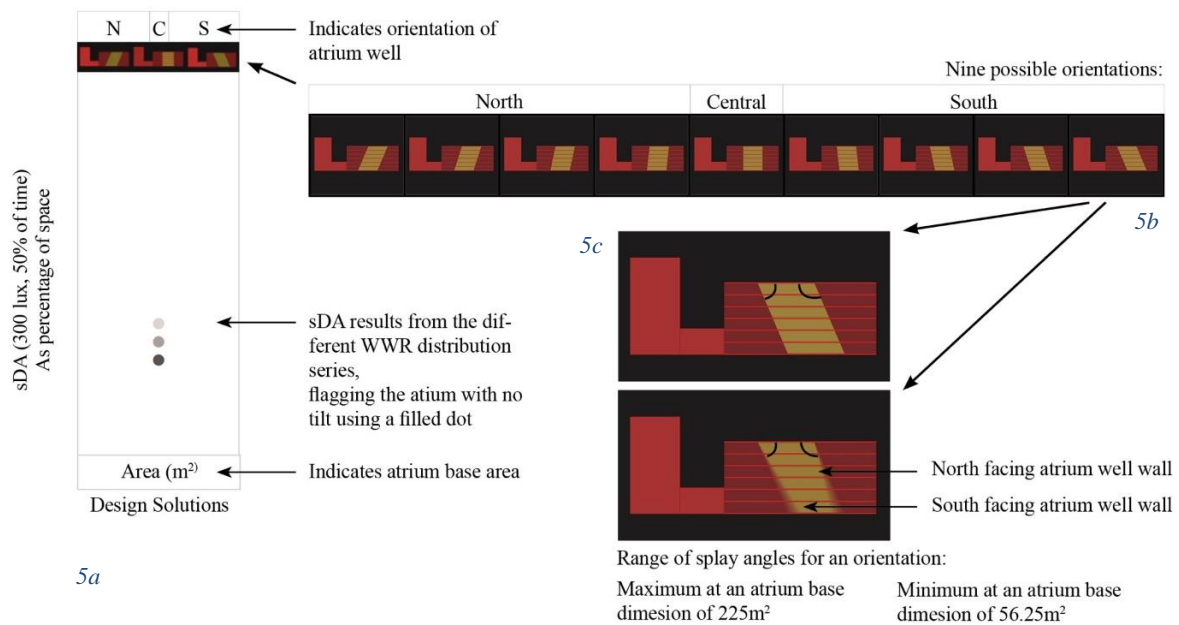relationships. Results are therefore presented and assessed in the following order:

Figure 5a. Graphic format to improve legibility of results; 5b. Atrium well orientations; 5c. Atrium well splay angle ranges

1.) Impact of atrium well geometry on sDA, with magnitudes assessed based on minimum
and maximum sDA values for each given floor area (Figure 6)

2.) Impact of WWR distribution on sDA, with magnitude assessed based on minimum and
maximum sDA ranges across the different WWR in each given floor area (Figure 7)

3.) Impact of atrium orientation on sDA, with magnitude assessed based on minimum and
maximum sDA ranges across the different orientations for each WWR option in each
given floor area (Figure 8)

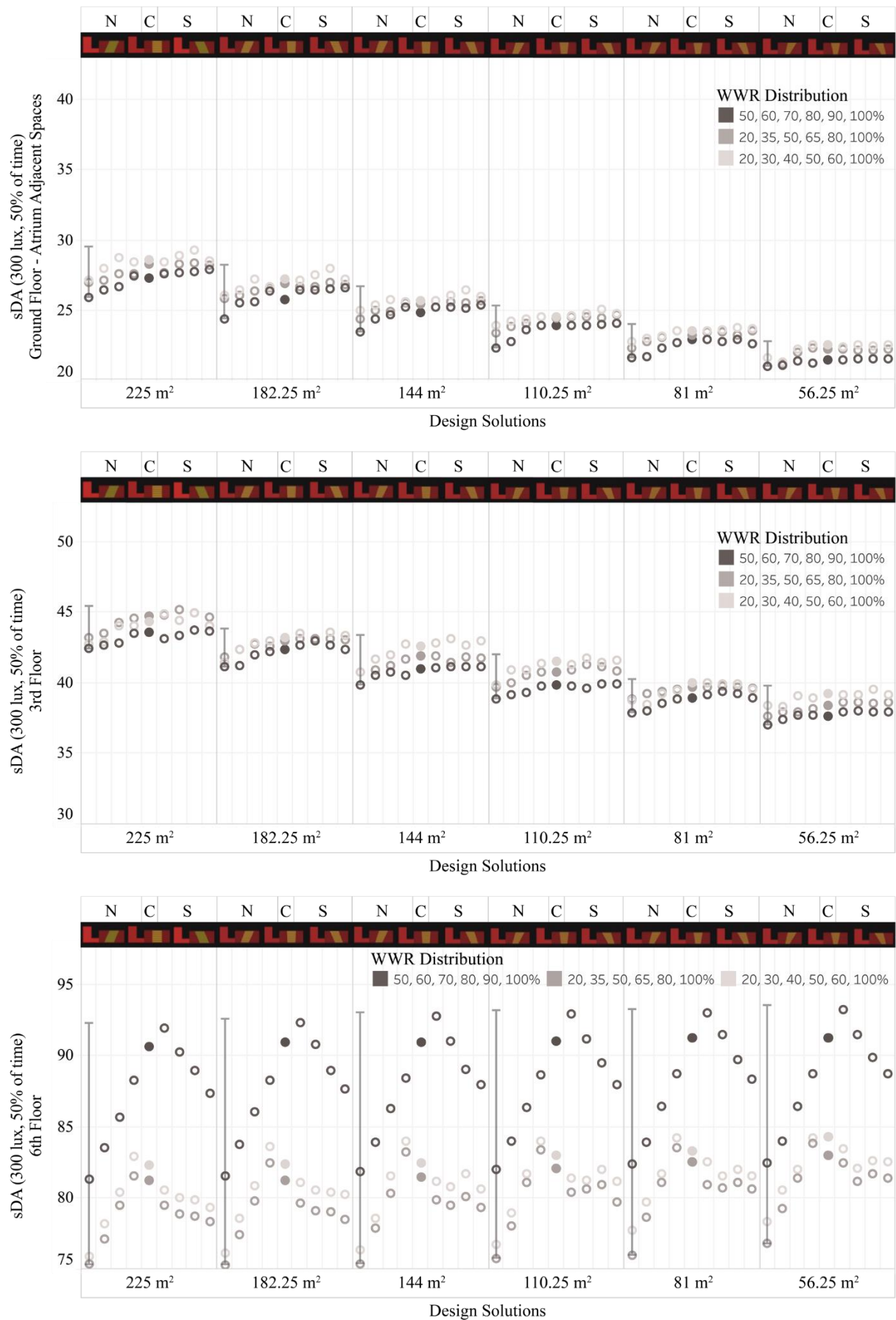4.) Combined impact of all design changes on sDA across all floors

Figure 6. sDA performance for atrium adjacent spaces: ground floor, 3rd floor, and 6th floor.

3.1 Impact of Atrium Well Geometry on sDA

For the ground floor, the larger the atrium base area, the higher the sDA levels in atrium adjacent spaces. This is true for the third floor, but not for the upper floor.

On the ground floor, sDA within a given atrium base area varied between 26 and 29% for the largest atrium base area and between 21 and 23% for smallest atrium base area (as indicated in Figure 6). This pattern is the same on the third floor, with sDA ranging between 42 and 45% and between 37 and 40 % for the largest and smallest atrium base areas respectively. From the 5th floor, this pattern starts changing, therefore sDA on the 6th floor ranged between 75 and 92 % for the largest atrium base area and increased to sDA between 77 and 93% for the smallest atrium base area. These magnitudes illustrate that a change in the atrium base floor area has the largest impact on the 3rd floor rather than the ground floor, with the smallest impact and a reverse effect on the top floor.

Pattern and magnitude changes are a product of a combination of an increase in room depth on lower floors (due to a reduction in the atrium well area), the depth of daylight penetration into the atrium well (due to a change in the atrium splay angles) and an increase in the effect of overshadowing from neighboring buildings towards lower floors. Starting from the 5th floor, the visible sky area increases with the splay angle, exposing larger portions of the atrium walls to the open sky. This improves daylight performance despite a slight increase in room depth.

3.2 Impact of WWR distribution on sDA

Figure 7 shows the maximum and minimum ranges in sDA for the different WRR options on the top floor. The WWR distribution series starting with 50% showed significantly higher sDA in comparison to both WWR distribution series starting with 20%, which showed very similar results to each other. Changing the WWR distribution shows less of an

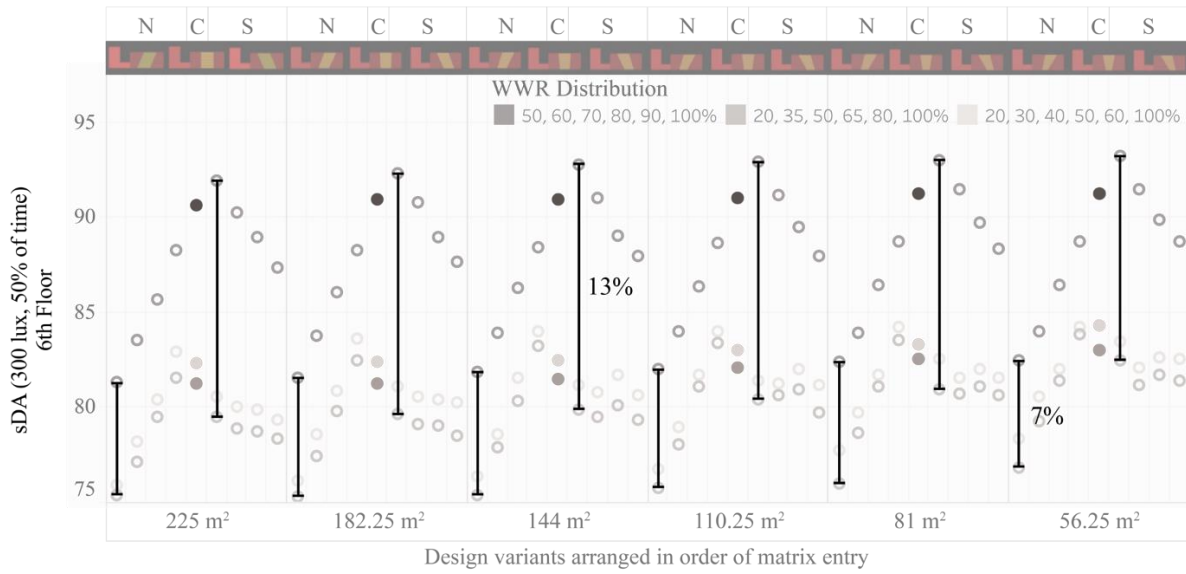impact on sDA when the atrium well is northward-oriented.

Figure 7. Maximum and minimum sDA ranges for WWR options on the 6th floor

On the top floor, the maximum range of variations in sDA was 13% whereas the minimum range was 7%. Maximum ranges occurred for solutions with a slight southern orientation and minimum ranges occurred for atria with the northernmost orientation. On the top and fifth floor, the 50% WWR distribution series consistently performed better. This pattern changed on the third and ground floors as the WWR distribution series of 20, 30, 40, 50, 60, 100% tended to perform better than the others. The range of variation in sDA based on WWR is much lower on the third and ground floors (as shown in Figure 6), with a difference lower than 2.3%. Despite being small, this difference does matter because it accounts for around 28m^2 (ground floor), meaning additional daylight is provided to the otherwise under lit areas in the proximity of the atrium well, thus making them more suitable to accommodate work environments.

A reduction in window area significantly diminished sDA results on the top floor improve sDA in the lower floors. This is because the presence of larger opaque surfaces on the upper floors increased the reflected light in the atrium well as a whole. This impact is particularly noticeable for the third floor in which the majority of design solutions with

65% WWR underperformed design solutions with 50% WWR, a result that might look counter intuitive for a designer. The turning point and exception to this can be found in design solutions with an atrium base area of 225m^2 from which the increase in reflected daylight could not offset anymore the additional access to daylight provided by larger window areas.

It is important to notice that this shift in patterns will be affected by the number of simulation ambient bounces. The higher the number of bounces, the deeper and further daylight will travel into atrium adjacent spaces. In addition, an increase of daylight levels in lower floors can also be achieved by increasing the reflectance of materials in the atrium well. Since both settings can heavily affect sDA on lower floors, further studies are needed to validate realistic settings for climate-based daylight simulations in atrium buildings.

3.3 Impact of Orientation on sDA

On all floors and across all design solutions, the northmost orientation showed the weakest sDA performance. The optimum orientations however varied.

On the top floor, the WWR distribution series starting with 50% showed a different optimum orientation than both WWR distribution series starting with 20%, which showed very similar results to each other. The optimum for the 50% WWR distribution series was found in slightly southern oriented atriums whereas the optimum for the other two WWR series were found in a slightly northern orientation. This pattern remained consistent across all atrium base areas. On the third and ground floor, the optimum orientation was southward for all WWR distribution series. One difference between these two floors was that the optimum orientations on the ground floor were more steeply oriented towards south than third floor optima. The turning point for optimum orientation changes from south to

north on the fifth floor, where a steeper northward orientation consistently provided the highest sDA for all WWR distribution series.

Figure 8 shows sDA variation for the different orientations on the top floor per WWR distribution series for each given atrium base area. The maximum range of variation, 11% sDA, was found in the 50% WWR distribution series and the minimum range, 6% sDA, in the 20, 30, 40, 50, 60, 100% WWR distribution series. The range of variation in sDA based on orientation is much lower on the third and ground floors (as shown in Figure 6), with a difference lower than 2.5% sDA.
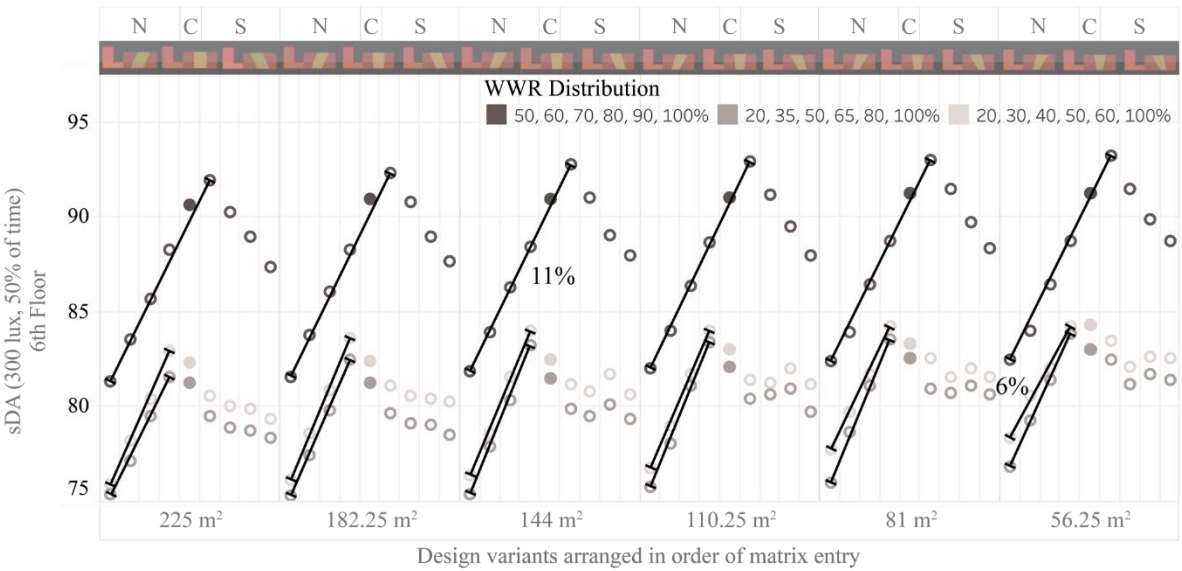

Figure 8. Maximum and minimum sDA ranges for Orientation on the 6th floor

It is important that orientation is understood in association with the splay angles of the atrium well walls. For each of the nine orientations (Figure 5b), the resulting splay angles vary with the size of the atrium base area (as displayed in Figure 5c). The combination of Figures 5b and 5c are therefore presented as a range of splay angles in Table 5. The splay angles were measured at the north-facing and south-facing atrium well walls (Figure 5c).

Table 5 shows the splay angles of the orientations that most commonly resulted in the highest sDA on the top, third, and ground floor with the turning point described for the

fifth floor. The northward orientations are, for the most part, associated with an obtuse splay angle of the north-facing atrium well wall and an acute splay angle of the south-facing atrium well wall. This is vice versa the case for the south ward orientations. One exception are the slightly north/ southward orientations (underlined figures in bold, Table 5): here the atrium design solutions with an atrium base area of 110.25m^2 and lower have acute splay angles on both the north- and south-facing atrium well walls.

Table 5. Splay angles of design solutions grouped according to orientation; results of best performing orientations marked with in red

Orientation	North-most	North	North	North	Central	South	South	South	South-most
Splay angle of north-facing wall	113.2 to 102.6°	107.8 to 96.7°	102.1 to 90.8°	96.1 to **84.8°**	90 to 78.9°	83.9 to 73.2°	77.9 to 67.9°	72.2 to 62.9°	66.8 to 58.4°
Splay angle of south-facing wall	66.8 to 58.4°	72.2 to 62.9°	77.9 to 67.9°	83.9 to 73.2°	90 to 78.9°	96.1 to **84.8°**	102.1 to 90.8°	107.8 to 96.7°	113.2 to 102.6°

| | 5th Floor | 6th Floor (20%WWR) | 6th Floor (50%WWR) | 3rd Floor | Ground Floor |

The smaller the window area and the lower the floor level, the lower the impact of orientation on sDA. This is noticeable when comparing design solutions with 50 and 20% WWR on the top floor and results on top floor to those on the lower floors (Figure 6). Thus, spaces with greater availability of daylight were more affected by the choice of orientation.

Southward oriented atria typically showed higher sDA levels below the fifth floor. The optimum orientation changed more steeply towards south in lower floor levels. This is because, to perform better, the lower floor levels need deeper daylight penetration into the atrium well. This can be achieved by aligning the splay angles with the solar altitude, which

as consequence, increases reflected daylight into atrium adjacent spaces. As floors go up, the atrium adjacent spaces need to be more perpendicular with the solar altitude in order to increase direct daylight penetration and reflected daylight from atrium well walls. In addition to that, perpendicular walls also favour reflected daylight from the atrium base to reach upper floors.

Less intuitive results were found on the top two floors where optimal orientations vary. Especially on the top floor where north/ south orientations perform better for different WWR options, the relationship between orientation and splay angles becomes difficult to entangle. The derivation of conclusions would therefore need a more detailed analysis of the spatial distribution of daylight and of the climate data itself as well as further validation of the results. Nonetheless, the following lines of argument provide possible explanations for the presented results:

On the fifth floor, there was a shift in pattern as north oriented atria displayed higher sDA levels regardless of the WWR. This situation also holds true for 20% WWRs on the top floor level. The higher sDA values for north oriented atria can be explained by several aspects: Northward orientation and acute splay angles of the south-facing atrium well wall expose more floor area in the south of the atrium towards the sky (top light rather than side light). At the same time, the south facing atrium well wall provides an orthogonal surface to prevailing solar angle thus enabling deeper daylight penetration into atrium adjacent spaces in the south. Additionally, more daylight is reflected from the south facing atrium well walls as the percentage of opaque surfaces is particularly high with the low WWR.

A few arguments also explain the higher sDA levels for the southward orientation on the top floor for 50% WWR: Southward orientation and acute splay angles of the north-facing atrium well wall expose more floor area in the north of the atrium towards the sky (top light rather than side light). At the same time, obtuse splay angles improve daylight

distribution (more diffuse light) and daylight levels in the south of the atrium (Laouadi 2004; Parent and Murdock 1989). The results would suggest that the improvements in daylight from obtuse angles of the north-facing atrium well wall are greater than from a perpendicular orientation towards south, given that the window area is large enough (in this case 50%).

Explanations could however also extend to reasons unknown to the authors. These arguments will therefore need to be investigated more closely in future work. Besides that, the current study used a simplified model with zero wall-thickness. Results may change, further shifting the optimum orientations when including wall-thickness in the simulation models.

3.4 Prediction of sDA across all floors

Figure 9 shows the total sDA performance across all floor levels (average weighted according to floor area). SDA within the design solution space ranged between 45 and 55% and therefore contained design variants that both meet and fail the 50% standard sDA threshold. The smaller the atrium base area, the lower the sDA. The WWR distribution series starting with 50% consistently outperformed the other two, which showed overlapping results. The optimum orientation across all floor levels was the same as the one shown previously for the top floor, i.e. with a slightly south and slightly north orientation showing the highest sDA for WWR distribution series starting with 50% and 20% respectively.
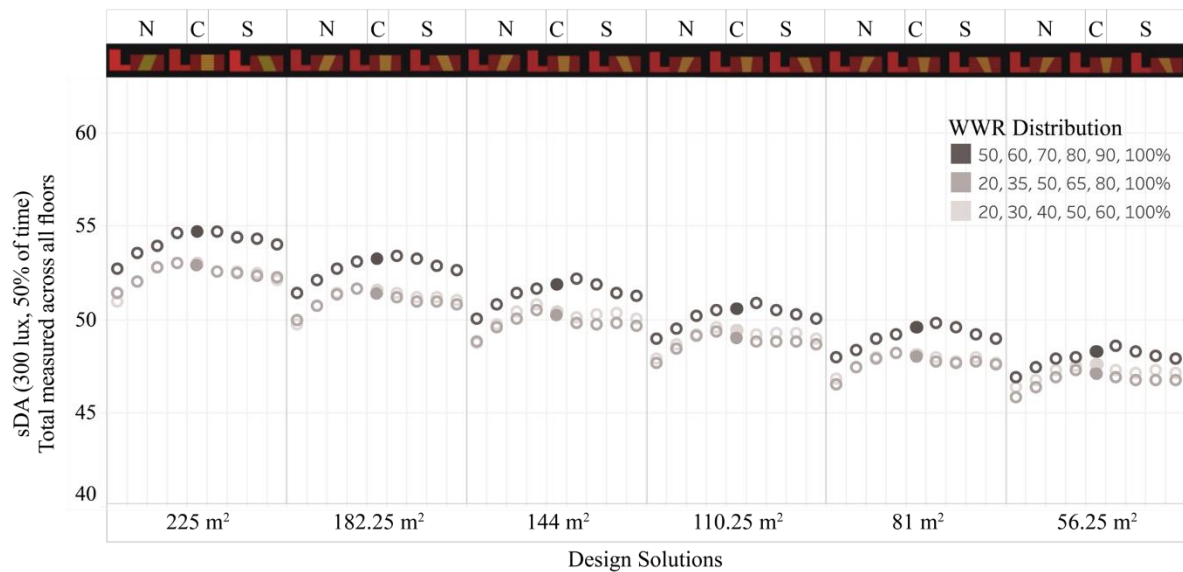
Figure 9. sDA performance across all floor levels

The sDA results ranged between 51 and 55%, and 46 and 49% sDA for the largest and smallest atrium base area respectively. The variation between WWR distribution options as well as orientations was below 3% sDA. The atrium base area therefore showed the biggest impact on the overall sDA of the building.

The highest sDA relating to WWR distribution was seen for the WWR distribution series starting with 50%, a result only representative only of the top two floors. The highest sDA relating to orientation was seen on slight north/south orientations, again a result only representative of the top floor. This means the top floor is skewing the results, making them unsuitable to develop guidelines for design decisions. This becomes even clearer when considering that, on the top floor, even the weakest design variants achieved sDA higher than 75%, a threshold indicating 'preferred daylight sufficiency' (Heschong Mahone Group 2003; IESNA 2012), meaning that the 'worst case' design choices, as suggested by the combined performance, do not negatively affect daylight levels on the top floor. When looking at the individual floor results however, these design choices do negatively affect daylight on the lower floors, where the availability of daylight is especially critical. This

leads one to conclude that it is important to consider the impact of design choices locally (i.e. per floor or even per room) rather than simply globally (i.e. for the whole building).

4. Time performance after integrating ANNs

The comparison of time performance between ANNs and the conventional daylight simulation is done by comparing the actual elapsed time. On a 2.6 GHz Intel Core i9, one daylight simulation took around three hours per floor. The ANN models were trained using data from 45 out of 162 simulations. The validation of ANN prediction accuracies was undertaken for the ground, 3rd and 6th floors using another 21 simulations per floor. The ANN predictions therefore substituted 96 out of 162 simulations on the ground, 3rd and 6th floor and 117 simulations on all other floors (ANNs replaced 66% of simulations). After deducting ANN training and optimization time for a 4-layered neural network with 38-40 neuron in the first hidden layer and 19-20 neurons in the second hidden layer, the total simulation time was reduced by 65%. This is a conservative calculation and time intensity can further be alleviated by reducing the number of simulations and the size of the network architecture. Using 36 out of 162 simulations for ANN training, overall simulation time can further drop by 71% without much impact on prediction accuracy (Lorenz *et al.* 2019).

5. Conclusions and future work

The study explores the effectiveness of using Artificial Neural Networks (ANN) in the early stages of daylight design. Two types of results are presented. The first relates to understanding the possibilities of using ANNs as a method to explore daylight design as surrogates for simulations, whereas the second provides insights on the subtleties involved in daylight design of buildings with a central atrium. In this respect it is important to say that simulation results were not validated against real world readings due to the complexity

of replicating annual climate data. The systematic errors of the simulation employed to train the ANN are therefore certainly mirrored by the ANN and allows to draw exclusively general conclusions.

A reduced sample of simulations from the solution space enabled the ANNs to predict daylight results of the entire design space. At the same time, ANNs were able to display heterogeneity of performance across the design solution space and the non-linear interactions between different parameters influencing daylight performance. For instance, they predicted a change in the daylight performance pattern in the 3rd floor considering atrium orientation and WWR. Such 'unforeseeable' results, as provided by the ANNs, provide valuable information for evaluating the different design configurations and design choices.

The analysis of daylight results enabled insights on the subtleties involved in daylight design of buildings with a central atrium. From comparing the variation of daylight performance on different floors with different WWRs and orientations, one can see there is no single optimal solution for the best daylight exploitation. Careful considerations in relation to the combination of these parameters need to be taken on board, especially so that lower floors reach compliance. Also, when planning building layout, sDA results can be taken used to determine the location of spaces required to comply with regulation thresholds.

The aim of this study was to alleviate the time intensity of a brute-force approach while harbouring its benefits for design exploration. The 65% time savings gained using ANNs rather than conventional daylight simulations enabled all possible instances in the parameterised design solution space to be examined. This brute force approach empowers designers to make informed decisions by uncovering trends and patterns in daylight performance. It also maintains the flexibility to change design objectives post optimisation

as all partial results remain available. To illustrate, the designer can search for design variants that achieve increased daylight levels on the lower floors rather than a higher overall building daylight performance (total across all floors). In comparison, an algorithm that selectively evolved the available design solutions towards improving the overall building daylight performance will have omitted the design choices that result in increased daylight levels on the lower floors but therefore lower overall building daylight levels (i.e. the design solutions with lower atrium well glazing area but higher reflected daylight). Brute force has been pushed aside by optimisation techniques for being computationally intensive, which has reduced the universe of choice for designers. Due to the achievable time-savings, ANNs offer a possibility to readapt the brute-force approach into the design process.

The obtained ANN predictions were fed back to the Grasshopper model, where currently available plug-ins such as Design Explorer[2] and Design Space Exploration[3] provide the possibility to facilitate design exploration and user interaction with the results. Future work can focus on the following areas: (i) development of a plug-in to the architectural software (Grasshopper[4] or Dynamo[5]) in order to automate model parametrisation, ANN training feature extraction, ANN training and validation, and ANN optimisation; (ii) automation of the transfer of ANN results to existing interfaces for visualisation and feedback, (iii) determination of information required by designers to ultimately achieve optimised solutions with improved building performance with regards to occupant well-being and environmental impact.

---

[2] *Design Explorer v2*. Tomasetti, T., *CORE Studio*. Last updated by Peng, M. (2019). Available at: https://tt-acm.github.io/DesignExplorer/ (accessed Oktober 21, 2019).

[3] *Design Space Exploration*. *Digital Structures*. Available at: https://www.food4rhino.com/app/design-space-exploration#lg=1&slide=0 (accessed Oktober 21, 2019).

[4] *Grasshopper*. Rutten, D., *Robert McNeel & Associates*. Available at: https://www.grasshopper3d.com/page/download-1 (accessed Oktober 21, 2019).

[5] *Dynamo Studio*. *Autodesk.* Available at: https://www.grasshopper3d.com/page/download-1 (accessed Oktober 21, 2019).

Acknowledgements

References

Aschehoug, O. (1992) 'Daylight in glazed spaces', *Building Research & Information*, 20(4), pp. 242–245.

Bhavani, R. G. and Khan, M. A. (2009) 'An intelligent simulation model for blind position control in daylighting schemes in buildings', *Building Simulation*, 2(4), pp. 253–262.

Bodart, M. and De Herde, A. (2002) 'Global energy savings in offices buildings by the use of daylighting', *Energy and Buildings*, 34(5), pp. 421–429.

Cole, R. J. (1990) 'The effect of the surfaces adjoining atria on the daylight in adjacent spaces', *Building and Environment*, 25(1), pp. 37–42.

Coley, D. A. and Crabb, J. A. (1997) 'An artificial intelligence approach to the prediction of natural lighting levels', *Building and Environment*, 32(2), pp. 81–85.

Conraud-bianchi, J. (2008) *A Methodology for the Optimization of Building Energy, Thermal, and Visual Performance*.

EFA (2014) 'EFA Daylight Design Guide Rev02', (January), pp. 1–10.

Eltaweel, A. and Su, Y. (2017) 'Parametric design and daylighting: A literature review', *Renewable and Sustainable Energy Reviews*, 73(October 2016), pp. 1086–1103.

Erlendsson, Ö. (2014) *Daylight Optimization : A Parametric Study of Atrium Design*. Royal Institute of Technology Stockholm, Sweden.

Figueiro, M. G. *et al.* (2017) 'The impact of daytime light exposures on sleep and mood in office workers', *Sleep Health*. National Sleep Foundation., 3(3), pp. 204–215.

Fonseca, R. W. Da, Didoné, E. L. and Pereira, F. O. R. (2013) 'Using artificial neural networks to predict the impact of daylighting on building final electric energy requirements', *Energy and Buildings*. Elsevier B.V., 61, pp. 31–38.

Forrester, A. I. J. and Keane, A. J. (2009) 'Recent advances in surrogate-based optimization', *Progress in Aerospace Sciences*, 45(1–3), pp. 50–79.

Heschong, L., Wright, R. L. and Okura, S. (2002) 'Daylighting Impacts on Retail Sales

Performance', *Journal of the Illuminating Engineering Society*, 31(2), pp. 21–25.

Heschong Mahone Group (2003) *System Design*, *Modular Skylight Systems for Suspended Ceilings. Project 5.3.5*.

Heschong Mahone Group (2012) *Daylight Metrics - PIER Daylighting Plus Research Program Final Report to the California Energy Commission*. CA, USA.

Hu, J. and Olbina, S. (2011) 'Illuminance-based slat angle selection model for automated control of split blinds', *Building and Environment*. Elsevier Ltd, 46(3), pp. 786–796.

IESNA, I. E. S. (2012) 'LM-83-12 IES Spatial Daylight Autonomy (sDA) and Annual Sunlight Exposure (ASE)', *New York, NY, USA: IESNA Lighting Measurement*.

Ipeck, E., Mckee, S. A., Caruana, R. and Schulz, M. (2006) 'Efficiently Exploring Architectural Design Spaces via Predictive Modeling', in *ACM SIGOPS Operating Sysems Review*. CA, USA, pp. 195–206.

Kim, W., Jeon, Y. and Kim, Y. (2016) 'Simulation-based optimization of an integrated daylighting and HVAC system using the design of experiments method', *Applied Energy*. Elsevier Ltd, 162, pp. 666–674.

Laouadi, A. (2004) 'Design with SkyVision : a computer tool to predict daylighting performance of skylights', in *CIB 2004 World Building Congress*. Toronto, Canada, pp. 1–11.

Lorenz, C.-L. *et al.* (2018) 'Artificial Neural Network-Based Modelling for Daylight Evaluations', in *Symposium on Simulation for Architecture + Urban Design*. Delft, The Netherlands.

Lorenz, C.-L. *et al.* (2019) 'Machine Learning in Design Exploration: An Investigation of the Sensitivities of ANN-Based Daylight Predictions.', in *CAAD Futures Conference Proceedings*. Deajeon, South Korea.

Lorenz, C.-L. and Jabi, W. (2017) 'Predicting Daylight Autonomy Metrics Using Machine Learning', in *International Conference for Sustainable Design of the Built Environment*. London, U.K.

Maesano, C. and Annesi-Maesano, I. (2012) 'Impact of Lighting on School Performance in European Classrooms', *Clima2016, doi 10*, pp. 1–14.

Magnier, L. and Haghighat, F. (2010) 'Multiobjective optimization of building design using

TRNSYS simulations, genetic algorithm, and Artificial Neural Network', *Building and Environment*. Elsevier Ltd, 45(3), pp. 739–746.

Mardaljevic, J. (2008) 'Climate-Based Daylight Analysis for Residential Buildings Impact of various window configurations , external obstructions , orientations and location on useful daylight illuminance', *IESD Technical report*. De Montfort University. Available at: http://www.thedaylightsite.com/.

Marquardt, D. (1963) 'An Algorithm for Least-Squares Estimation of Nonlinear Parameters', *SIAM Journal on Applied Mathematics*, 11(2), pp. 431–441.

McNeil, A. and Lee, E. S. (2012) 'A validation of the Radiance three-phase simulation method for modelling annual daylight performance of optically complex fenestration systems', *Journal of Building Performance Simulation*, 6(1), pp. 24–37.

Parent, M. D. and Murdock, J. B. (1989) 'Skylight Dome Well System Analysis from Intensity Distribution Data', *Lighting Research & Technology*, 21(3), pp. 111–123.

Reinhart, C. F., Mardaljevic, J. and Rogers, Z. (2013) 'Dynamic Daylight Performance Metrics for Sustainable Building Design', *The journal of the illuminating Engineering Society of North America*, 3(1), pp. 7–31.

Reinhart, C. F. and Walkenhorst, O. (2001) 'Validation of dynamic RADIANCE-based daylight simulations for a test office with external blinds', *Energy and Buildings*, 33(7), pp. 683–697.

Samant, S. (2017) 'Atrium and its adjoining spaces: a study of the influence of atrium façade design Swinal Samant Atrium and its adjoining spaces: a study of the influence of atrium faç ade design', *Architectural Science Review*, 54(4).

Samuelson, H., Claussnitzer, S., Goyal, A., Chen, Y. and Romo-Castillo, A. (2016) 'Parametric Energy Simulation in Early Design: High-Rise Residential Buildings in Urban Contexts.', *Building and Environment, Vol. 101,* pp. 19–31.

Tresidder, E. (2014) 'Accelerated optimisation methods for low-carbon building design',

Veitch, J. A., Christoffersen, J. and Galasiu, A. D. (2013) 'Daylight and View through Residential Windows : Effects on Well-being', in *Residential dayligting and well-being*, pp. 1–6.

Wong, S. L., Wan, K. K. W. and Lam, T. N. T. (2010) 'Artificial neural networks for

energy analysis of office buildings with daylighting', *Applied Energy*. Elsevier Ltd, 87(2), pp. 551–557.

Zhao, H. X. and Magoulès, F. (2012) 'A review on the prediction of building energy consumption', *Renewable and Sustainable Energy Reviews*. Elsevier Ltd, 16(6), pp. 3586–3592.

Zhou, S. and Liu, D. (2015) 'Prediction of Daylighting and Energy Performance Using Artificial Neural Network and Support Vector Machine', *American Journal of Civil Engineering and Architecture, Vol. 3, 2015, Pages 1-8*, 3(3A), pp. 1–8.